

Importance of molecular shape for the overall stability of hydrogen bond motifs in the crystal structures of various carbamazepine type drug molecules

Aurora J. Cruz Cabeza,^a Graeme M. Day,^a W. D. Samuel Motherwell^b and William Jones^a

^aThe Pfizer Institute for Pharmaceutical Materials Science, Department of Chemistry, University of Cambridge, Lensfield Road, Cambridge CB2 1EW, UK.

^bCambridge Crystallographic Data Centre, 12 Union Road, Cambridge, CB2 1EZ, UK.

Abstract

Carbamazepine, a first generation anticonvulsant, is known to crystallize in various polymorphic forms, all of which exhibit an anti-carboxamide hydrogen bond dimer motif. Furthermore, unless cocrystallized with carboxylic acids, these dimers are also present in most crystal structures of the known carbamazepine solvates. On the other hand, two derivatives of the drug (oxcarbazepine and 10,11-dihydrocarbamazepine) have been reported to adopt hydrogen bond chain motifs in their crystal structures, whereas the epoxy derivative (10,11-epoxycarbamazepine) shows a third mode of hydrogen bonding - syn-dimers. In order to rationalize the differences in hydrogen bonding caused by the small changes in molecular structure, computational searches for the low energy crystal structures of these drugs were performed and hydrogen bond patterns in both the hypothetical and experimentally determined crystal structures were analyzed. In addition,

interactions energies between pairs of molecules were calculated using the SCDS-Pixel approach, which partitions the intermolecular interaction energy in its different contributions (Coulombic, polarization, dispersion and repulsion). The importance of overall molecular shape and the influence that this has on the hydrogen bond arrangements in these structures is emphasized.

Keywords: crystal structure prediction, molecular shape, hydrogen bonding, carbamazepine and carbamazepine derivatives.

1. Introduction

Carbamazepine (CBZ) is a first generation anticonvulsant used in the treatment of epilepsy and trigeminal neuralgia. Metabolized in the liver, the first step in its degradation consists of the oxidation of the C₁₀-C₁₁ double bond (Figure 1) to the carbamazepine 10,11-epoxide (ECBZ),¹ a metabolite responsible for some of the side effects associated with consumption of the drug.² The derivative 10,11-dihydro 10-oxo carbamazepine, known as oxcarbazepine (OXCZ), has been shown to have several advantages as a drug, including improved efficacy, tolerability and fewer side effects.^{3,4}

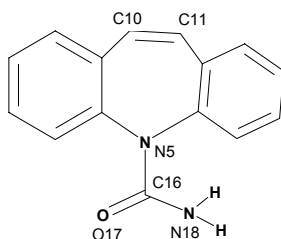


Figure 1. Sketch of carbamazepine and numbering of some of the atoms.

CBZ is not only an interesting system from a pharmacological view, but also as a model compound for the study of polymorphs,⁵ solvates⁶ and cocrystals.⁷ To date, however, no reports have appeared dealing with the possible polymorphs or cocrystals of CBZ derivatives such as ECBZ and OXCZ.* Four polymorphs are reported for carbamazepine: Form I⁵ ($P\bar{1}$, Cambridge Structure Database⁸ Refcode = CBZMZPN11), Form II⁹ ($R\bar{3}$, CSD Refcode = CBMZPN03), Form III¹⁰ ($P2_1/c$, CSD Refcode = CBMZPN01) and Form IV¹¹ ($C2/c$, CSD Refcode = CBZMZPN12). All the polymorphs exhibit similar hydrogen bonding: i.e. anti-carboxamide dimers (Figure 2). Furthermore,

* During preparation of the manuscript, a second polymorph of one CBZ derivative, 10,11-dihydrocarbamazepine (DHCZ), was reported. In this paper, where we refer to the crystal structure of DHCZ we mean the previously known $P2_1/c$ form, unless otherwise indicated.

unless cocrystallized with a carboxylic acid, most of the reported CBZ solvates show a similar hydrogen bond anti-dimer motif.⁷ Recently, however, crystal structure prediction studies for CBZ have suggested that both anti-dimers and chains are of comparable stability.^{6,12} Despite an extensive experimental screen using high throughput crystallization methods,⁶ no additional polymorphs were obtained and in particular none exhibiting the chain motif. Interestingly, we noticed that two derivatives of the drug, OXCBSZ ($P2_1/c$, whose crystal structure was only recently reported¹³) and 10,11-dihydrocarbamazepine¹⁴ (DHCBSZ) ($P2_1/c$, CSD Refcode = VACTAU01) exhibit chain motifs in their crystal structures (Figure 2). The epoxy derivative ECBZ¹⁵ (Pbcn, CSD Refcode = ZIPTEX) shows a third mode of hydrogen bonding: twisted syn-dimers (Figure 2).

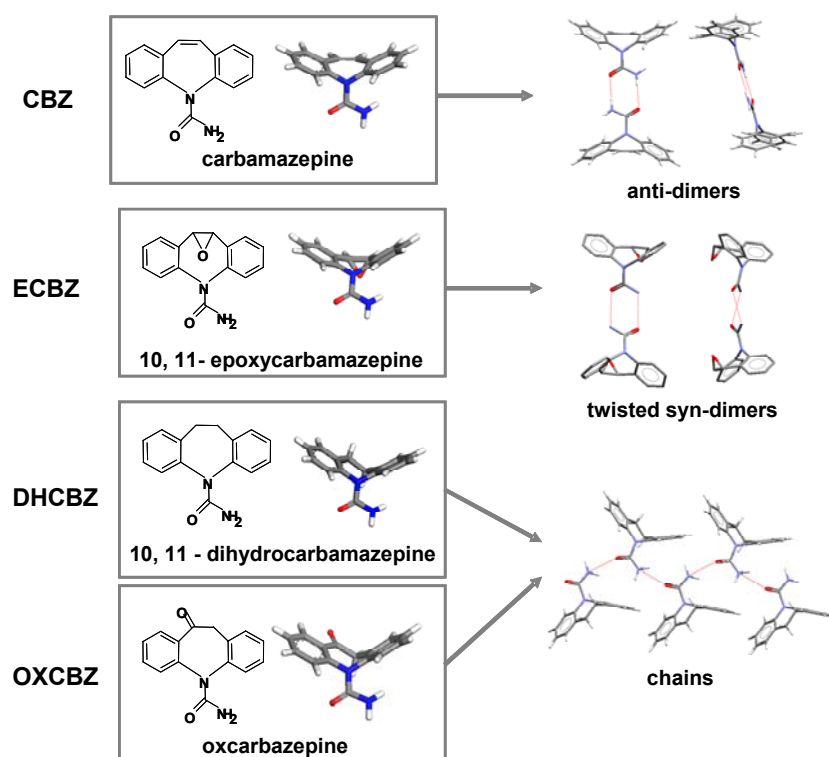


Figure 2. Carbamazepine (CBZ), 10,11-epoxycarbamazepine (ECBZ), 10,11-dihydrocarbamazepine (DHCBZ), and oxcarbazepine (OXCZ) molecular structures and hydrogen bond motifs observed in the crystals.

The questions we address here are: how can we explain the dramatic influences that small changes in molecular structure (remote from the hydrogen bonding functional group) have on the observed hydrogen bonding in the crystal structures and how “predictable” are the structures adopted by the various derivatives?

Crystal structure prediction¹⁶⁻¹⁸ (CSP) is a growing area of research whose main aim is to predict the observable crystal structures of a compound starting from only a knowledge of molecular connectivity. Such a powerful technique is of great applicability especially in pharmaceutical sciences and other areas (eg. fine chemicals and pigments). If the crystal form used for drug delivery is not the most stable, phase transitions may occur to another polymorph with unpredictable and potentially serious changes in physical properties.¹⁹⁻²¹ In this study, we present crystal structure prediction calculations for ECBZ, DHCBZ and OXCZ and compare the results with those recently reported for CBZ itself.¹² Of special interest are the CSP calculations for OXCZ, as it is a second generation antiepileptic drug currently in use and no studies have been reported on the stability of the observed crystal structure or tendency for polymorphism. Additionally, the distributions of hydrogen bond patterns, along with other molecular interactions are analyzed. SCDS-Pixel^{22,23} calculations of the strengths of these competing interactions are used to rationalize their effect on the observed hydrogen bonding on the various crystal

structures. Finally, we discuss the importance of molecular shape and its influence on the hydrogen bonding interactions for these molecules in the crystal structures.

2. Computational Methods

Molecular models. All molecular models were treated as rigid during the crystal structure search and lattice energy minimizations. The initial molecular structures were taken from density functional theory (DFT) isolated molecule geometry optimizations using the code *Dmol3* as implemented in the Accelrys package *Materials Studio*,²⁴ using the PW91 functional²⁵ and the double numerical polarised (DNP) basis set.²⁶

Model potential. The repulsion-dispersion contributions to the intermolecular potential were evaluated using the W99 empirically derived atom-atom potential parameters²⁷⁻²⁹ and interactions were summed to a 15 Å cutoff. The centre of interaction for all hydrogen atoms was shifted 0.1 Å along the X-H bond (X= C, N, O) towards the heavy atom; X-H distances were shortened by 0.1 Å after DFT optimization.

Electrostatic models. Electrostatic contributions to the intermolecular potential were calculated from two models of the molecular charge distribution: atomic charges and atomic multipoles. Atom centred point charges were derived to reproduce the molecular electrostatic potential (ESP charges)^{30,31} using the fitting procedure implemented in *Dmol3*. Atomic multipoles up to $l=4$ (charge, dipole, quadrupole, octupole and hexadecapole) were obtained by performing a Distributed Multipole Analysis³² of a B3P91/6-31G(d,p) electron density using the *CADPAC* code.³³ All charge-charge,

charge-dipole and dipole-dipole interactions were evaluated using Ewald summation, while higher order terms (up to R^{-5}) were summed to a 15 Å cutoff on whole molecules.

Crystal structure prediction. Crystal structures were generated in ten of the most common space groups ($P2_1/c$, $P\bar{1}$, $P2_12_12_1$, $P2_1$, $C2/c$, $Pbca$, $Pnma$, $Pna2_1$, $Pbcn$ and $R\bar{3}$) using the simulated annealing algorithm of Karfunkel and Gdanitz³⁴⁻³⁶, as implemented in the Accelrys *Polymorph Predictor* (PP) module of the Cerius² software suite.³⁷ Searches were carried out with one molecule in the asymmetric unit ($Z'=1$), followed by lattice energy minimization (W99 + ESP charges) and clustering, to remove identical structures. Up to four independent searches were performed within each space group until the generation of structures converged. This initial clustering of structures was performed using the algorithm implemented in the Cerius2 software.³⁶ The simulated annealing adjustable parameters were taken from previous studies.³⁸

Refinement of the calculations. As described in a recent publication,¹² amide pyramidalization is an important flexibility problem to consider in crystal structure prediction. For consistency in the methodology and improvement of the calculations, amide pyramidalization was considered in the same way as reported recently in our study for CBZ.¹² For further details and a diagram of the methodology see supplementary information. Final results presented here correspond to crystal structures which were lattice energy minimized with the molecular model showing the optimal amide geometry (in each particular crystal structure) using the W99 potential (for the description of

dispersion and repulsion) and the atomic multipole model (for the description of the electrostatics) using the program *DMAREL*.³⁹

Structure Comparison and Final Clustering. The *COMPACK*⁴⁰ algorithm was used for the final clustering and comparison of the computer generated and the experimentally observed crystal structures (taken from the Cambridge Structural Database⁸) with a tolerance of 0.15 Å on atomic separations in a coordination sphere of 14 molecules.

Synthon calculations –SCDS Pixel method. The valence electron densities of the molecular models were calculated with the package Gaussian at the MP2/6-31G** level of theory using appropriate box sizes and steps of 0.08 Å in the calculations. Pixels were then condensed into super pixels. Molecular clusters, taken from the various *DMAREL* minimized crystal structures, were generated by using the appropriate crystal symmetry operations. Single point energy calculations of those molecular clusters were performed using the parameters described by Gavezzotti.⁴¹

3. Results

3.1. Similarities and dissimilarities of the molecular structures in the experimentally observed crystals

The main chemical differences between the molecular structures of CBZ and its derivatives are located in the azepine ring at carbons 10 and 11. While those atoms are double bonded in CBZ, they are epoxidated in ECBZ (the oxygen of the epoxide lying below the azepine ring), hydrogenated in DHCBZ, and carbonylated at C10 and hydrogenated at C11 in OXCBZ. The four derivatives are therefore chemically very different around the azepine ring but none exhibit any extra hydrogen bond donors, although the carbonyl in OXCBZ could act as hydrogen bond acceptor.

From the point of view of the molecular shape, ECBZ retains the symmetry and the shape of the azepine ring and is superimposable on the CBZ molecular structure (Figure 3), although the extra oxygen of the epoxy function constitutes an important change in terms of shape in the region below the azepine ring. By comparison, however, there is a clear break in the symmetry of the azepine ring in the other two derivatives and therefore a distortion in the shape of the “butterfly” ring system. DHCBZ and OXCBZ themselves are almost perfectly superimposable.

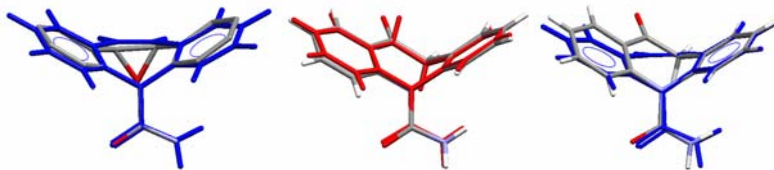


Figure 3. Superposition of the molecular structures of: a) CBZ (blue) and ECBZ; b) DHCBZ (red) and OXCBZ; and c) CBZ (blue) and OXCBZ. The molecular structures were taken directly from the experimentally solved crystal structures: CSD refcodes CBMZPN02, ZIPTEX , VACTAU and the crystal structure of oxcarbazequine.

3.2 Molecular models

When the symmetry of the azepine ring is broken in the molecular structures of DHCBZ and OXCBZ, the conformations obtained by a 180° rotation about the N5-C16 bond (Figure 1) are no longer related by inversion. As a result, two molecular minima with different energies can exist (we denote them as SYN and ANTI, Figure 4). The SYN conformations are those where the NH₂ groups are located on the same side as C10 (see Figure 1) whereas the ANTI conformation represents the opposite arrangement. In both cases, the SYN conformations are less stable than the ANTI conformations by 1.67 kJ/mol and 4.17 kJ/mol for DHCBZ and OXCBZ respectively (based on DFT calculations). Crystal structure prediction calculations using the ANTI or the SYN conformations would give rise to two completely different sets of crystal structures. After two independent crystal structure searches with each conformer, the most stable generated crystal structures for the SYN sets were located 7 kJ/mol and 5 kJ/mol higher in total energy than the most stable crystal generated with the ANTI conformations, for DHCBZ and OXCBZ respectively (see supplementary information). The crystals generated with the SYN conformation were not, therefore, energetically competitive with those generated with the ANTI and were not considered further.

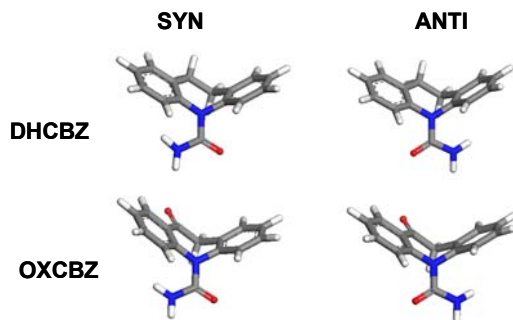


Figure 4. Molecular models of the ANTI and SYN conformations of DHCBZ and OXCBZ.

3.3 Crystal structure predictions

Crystal structures prediction results on the four systems are shown in Figure 6, where relative total energy (lattice + conformational) versus packing coefficient of the structures are classified by hydrogen bond motifs. All experimentally observed crystal structures (with the exception of Form I CBZ which has four molecules in the asymmetric unit) were successfully generated during the CSP calculations (circled structures, Figure 6). Nevertheless, their predicted stabilities, relative to the alternative computer generated crystal structures, vary between the four derivatives. For CBZ, the lattice energy calculations successfully predict two of the polymorphs (Form III and Form IV): their lattice energies are lowest amongst the predicted possibilities, along with an energetically competitive third structure, which has not yet been observed experimentally. On the other hand, Form II and the energy minimized Form I polymorphs were predicted not to be as stable (8.3 and 6.2 kJ/mol above the global minimum, for further discussions see reference 12). Predictions were not as successful for ECBZ, where the experimentally observed crystal structure was found to be almost 5 kJ/mol above the global minimum in energy. To date, no other polymorphs have been reported for this system, although predictions indicate that other more stable crystal structures are possible. Interestingly for DHCBZ, there are two very similar (but distinct) and almost isoenergetic generated structures (ranked number 2 and 3 in the final set of crystals) that match the experimentally observed crystal structure within the tolerances used in the structure comparison algorithm. These two apparent minima at 0 K would probably converge to one free energy minimum at higher temperatures and this “structure-delocalization” may result in a higher entropic contributions lowering its free energy relative to other

structures. Nevertheless, according to these results, there is still a hypothetical crystal structure predicted to be more stable (at 0 K) than the structure found in the CSD. In fact, while this paper was in preparation, the report of a new polymorph of DHC₂BZ was published.⁴² To our satisfaction, this new polymorph corresponded to the global minimum structure from our search. This polymorph shows the same type of hydrogen bonding as the previously known crystal structure. By way of contrast for the oxo derivative, OXC₂BZ, as the experimental crystal was predicted to be the most stable, with no other competitive structures in a range of 2.5 kJ/mol. This observation is important since it suggests that no polymorphs of competitive energy appear to be possible, suggesting that if this drug is commercialized with this form, no phase transformations to another polymorph would be expected.

Concerning the type of hydrogen-bond motifs (Figure 6), while both anti-dimers and chains are found amongst the most stable predictions for CBZ, chains are notably favoured for the DHC₂BZ and OXC₂BZ crystal structures (all the stable crystals up to 4 kJ/mol above the global minimum contain chains) (Figure 6). It is therefore not surprising that the experimentally observed crystal structures of both DHC₂BZ and OXC₂BZ show hydrogen bond chains. On the other hand, chains, anti-dimers and other types of motifs, where the epoxide oxygen is also involved as acceptor (see supplementary information), were found amongst the most stable of the ECBZ predicted structures. Unexpectedly, the experimental crystal structure shows syn-dimers (Figure 2) which are rarely found in any of the four sets of predictions (crossed squares in Figure 6).

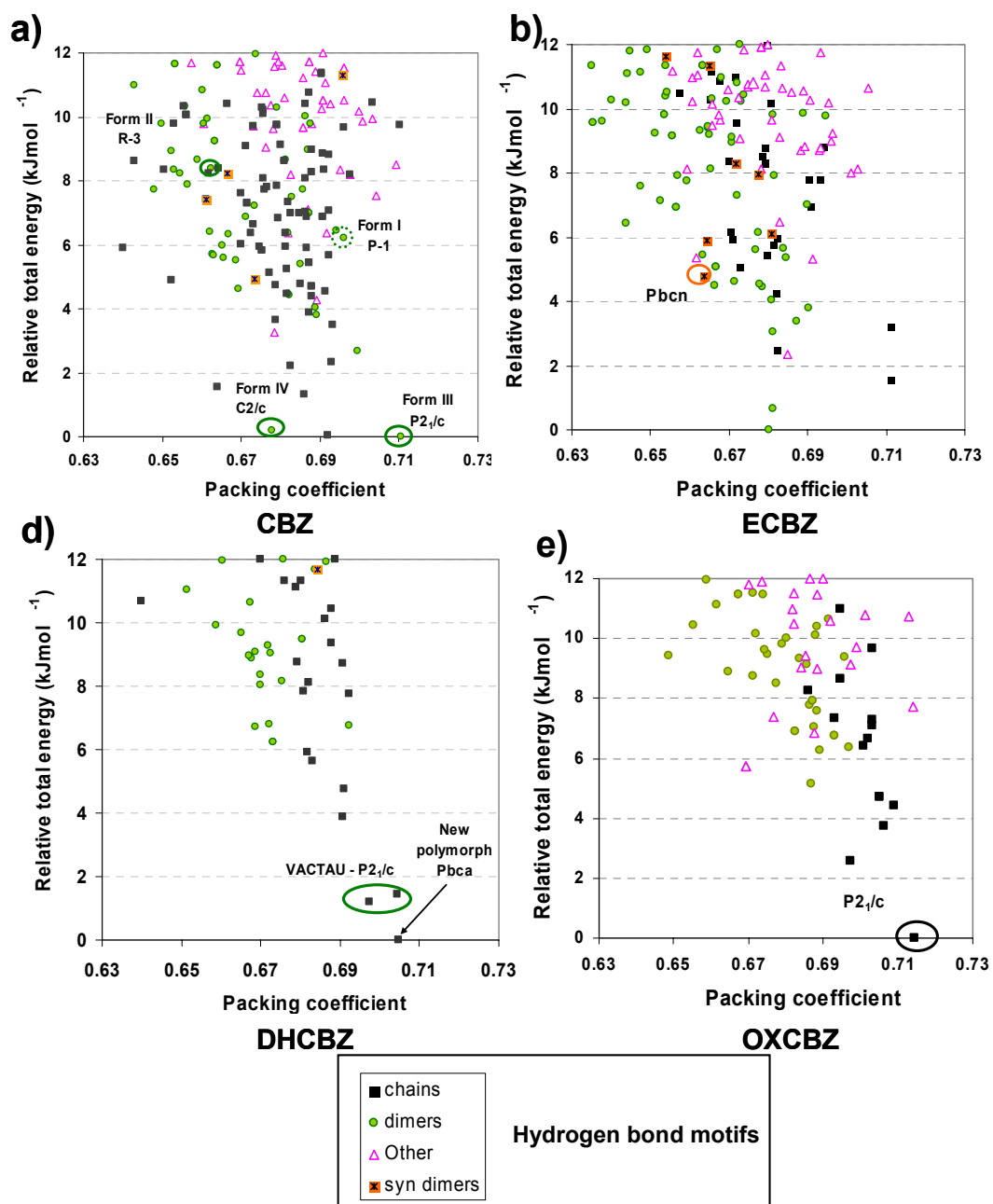


Figure 6. Final predictions classified by hydrogen-bonding motifs: a) carbamazepine,¹² b) epoxy-carbazepine, c) 10, 11-dihydrocarbamazepine and d) oxcarbazepine.

As a complementary analysis, the packing of the molecules in the different structures is also of great interest; there are two fundamental ways in which the azepine ring can pack: sandwich-herringbone and π - π stacking (Figure 7) [for further discussion on packing similarities in the observed CBZ crystal structures and some of its analogues see reference⁴³].

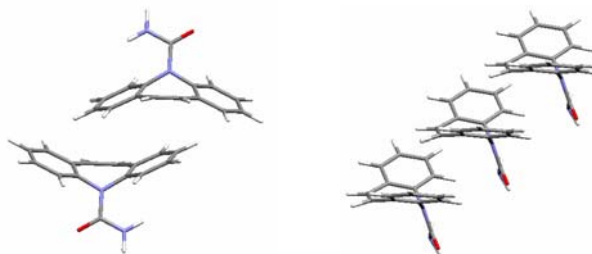


Figure 7. Types of recognizable packing of the azepine rings: sandwich-herringbone (left) and π - π stacking (right).

The three most stable structures predicted for carbamazepine (including Form III and Form IV) showed sandwich herringbone interactions between azepine rings whereas both Form I and Form II exhibited π - π stacking interactions (Figure 8). This π - π stacking interaction is not favourable in the case of epoxycarbamazepine, as the epoxyde oxygen lying below the azepine ring sterically prevents this contact, thus a sandwich-herringbone arrangement is the most commonly found amongst the most stable predicted crystal structures – in agreement with the experimentally observed crystal structure. Both the $P2_1/c$ polymorph of DHCBZ and the crystal structure of OXCBZ show π - π stacking. We observed that the best π - π stacked structures are both 4.7 kJ/mol more stable than the best sandwich-herringbone structures in this case. It is to be noticed that the recently discovered lower energy structure for DHCBZ has neither of these packing patterns.

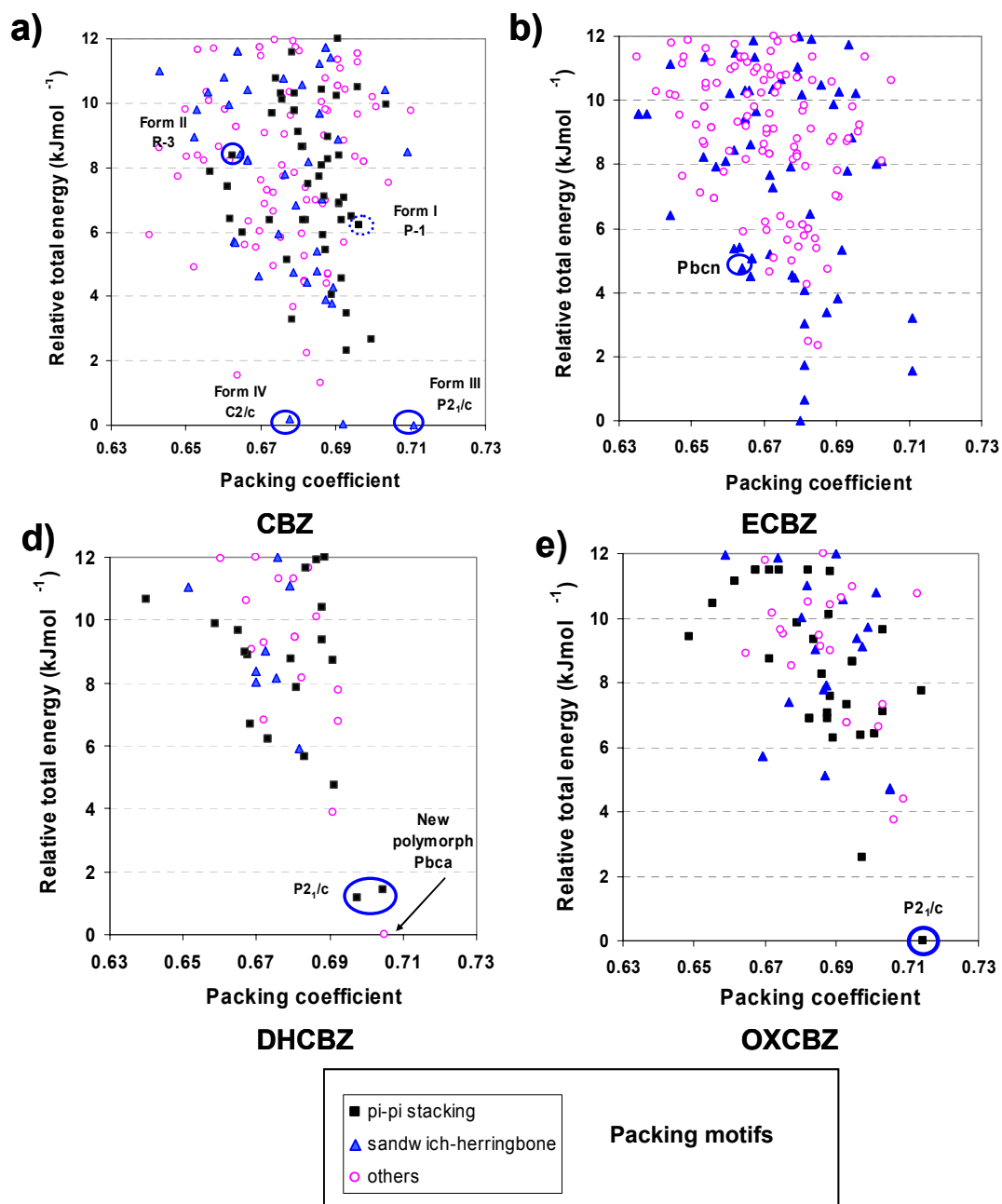


Figure 8. Final predictions classified by packing motifs: a) carbamazepine, b) epoxycarbazepine, c) 10, 11-dihydrocabamazepine and d) oxcarbazepine.

Finally, differences in the packing efficiencies of the four sets of crystal structures are also noticed. We find that OXCBZ packs more efficiently than the other derivatives with the observed crystal structure having a packing coefficient of 0.714. On the other hand, a large range of packing coefficients (from 0.677 to 0.710) is observed within the most stable crystal structures predicted for CBZ, of which the $P2_1/c$ polymorph is the most efficiently packed. For ECBZ, only two crystal structures pack in an exceptionally efficient way (black squares in Figure 6 at packing coefficients of 0.711). Neither of these structures has been observed but it would not be surprising if the most stable of them was obtained after crystallization under high pressure conditions. In fact high pressure has been used to access predicted crystal structures of other small molecules.⁴⁴ In comparing the packing efficiency of the different hydrogen bond motifs, we find that structures exhibiting hydrogen bond chains generally pack more efficiently than those containing dimers –with the exception of CBZ where the distinction in packing coefficient between chains and dimers is less clear.

3.4. Synthron calculations – PIXEL SCDS method

Although the geometries of molecular pairs taken from the crystal structures may not be energy minima when isolated from crystal forces, single point energy calculations of interaction energies in such pairs may help us determine which interactions are dominant in certain crystals and, therefore, which interactions are more important during crystal formation. For example, comparing the different interactions amongst polymorphic forms may be an important factor in understanding why a particular polymorph, over other possible ones, is observed under certain conditions. Also, a comparison of the interaction

energies of the same motifs found in the crystal structures of the different CBZ derivatives may clarify why chains are favoured in the crystal structures of some derivatives but not others.

We took molecular pair geometries from CBZ Form III (the most stable polymorph) and the known crystal structures of DHCBZ, OXCBZ and ECBZ. For comparison, we took molecular pairs from the most stable predicted hypothetical crystals with alternate hydrogen bonding to the observed structures: CBZ structure ranked 2 (the most stable chain), ECBZ global minimum (anti-dimers) and the most stable structures showing anti-dimers for DHCBZ and OXCBZ (ranked 8 and 6 respectively). Interaction energies calculated with the PIXEL method are summarized for these pairs in Table 1.

The calculated interaction energies of the anti dimer motifs are very similar for all four derivatives (~ -23 to -25 kJ/mol). However this is not the case for hydrogen bond chains, where the interaction energy is found to be favoured for DHCBZ and OXCBZ over CBZ by almost 4 kJ/mol. Chains and dimers in the CBZ crystals show comparable interaction energies (-24.8 and -24.7 kJ/mol respectively) whereas chains are clearly favoured over dimers for both DHCBZ (by ~ 4.5 kJ/mol) and OXCBZ (by ~ 6 kJ/mol). These energies are in line with the observations we made based on total lattice energies of the observed and predicted crystal structures and show that much of the energetic advantage for chains in DHCBZ and OXCBZ results from the strength of the interaction between hydrogen bonded molecules. For dimers, this interaction energy is dominated by the Coulombic contribution, which is weaker in the chains, but compensated for by a greater dispersion

energy (Table 1). On the other hand, anti-dimer interaction energies are also greatly favoured (by ~ 4.5 kJ/mol) over the syn-dimers in the ECBZ crystal structures.

Table 1. Interaction energies per hydrogen bond for the most stable (experimental or hypothetical) dimers and chains calculated using the PIXEL method.

Interaction		Crystal Structure	Packing	E_{coul} (kJ/mol)	E_{pol} (kJ/mol)	E_{disp} (kJ/mol)	E_{rep} (kJ/mol)	E_{total} (kJ/mol)
Anti dimers	CBZ	Form III	SH	-32.7	-11.3	-6.0	25.2	-24.8
	ECBZ	Hyp.Rank 1	SH	-29.2	-9.6	-6.1	21.8	-23.0
	DHCBZ	Hyp.Rank 8	π - π	-35.1	-11.6	-6.4	28.8	-24.2
	OXCBSZ	Hyp.Rank 6	SH	-27.2	-8.0	-5.8	17.8	-23.1
Syn dimers	ECBZ	Pbcn	SH	-17.8	-5.2	-5.5	9.4	-19.0
Chains	CBZ	Hyp.Rank 2	SH	-21.5	-9.8	-15.5	22.2	-24.7
	DHCBZ	P2 ₁ /c	π - π	-25.8	-11.7	-16.4	25.4	-28.6
	OXCBSZ	P2 ₁ /c	π - π	-25.5	-10.9	-16.4	23.8	-28.9

[†]SH=sandwich herringbone, π - π = π - π stacking of the azepine rings

4 Discussion

In light of the results described in sections 3.3 and 3.4, various noteworthy points can be addressed in an overall comparison of the four molecular systems.

4.1 On the possible latent polymorphism of CBZ derivatives

Limited by the type of calculations (static and at 0 K) and unable to consider kinetic effects, metastable polymorphs can not yet be predicted and growth condition effects on the relative stability of polymorphs cannot be studied computationally. Nevertheless, if the observed crystal structure happens not to be the global minimum in a CSP calculation, or many structures are found to be of very similar lattice energy, we

may expect polymorphism for the system. For example, we are confident that no thermodynamically more stable new polymorphs are to be expected for OXCBZ (as there are no competitive structures within approximately 3 kJ/mol) whereas for DHCBZ, we predicted a lower energy structure than the known crystal structure and this has now been experimentally observed. Similarly, polymorphism in ECBZ is expected according to the results of the CSP calculations, where many structures were found to be more stable in terms of lattice energy, and the PIXEL calculations show that the anti-dimer interaction is favoured over the syn-dimer one (Table 1).

On the other hand, we also notice differences in the density of generated structures (ie. the number of energy minima in a certain energy range above the global minimum) for the various derivatives; while many energetically competitive crystal structures are generated for CBZ and ECBZ (the two molecules where symmetry around the azepine ring is maintained), the number of generated structures of low energy for DHCBZ or OXCBZ (the two molecules where symmetry around the azepine ring is broken) is much lower. To what extent is molecular shape, or molecular symmetry, determining the number of low energy packing possibilities and in a way its potential polymorphism? Could we then state that OXCBZ is less likely to be polymorphic than ECBZ? Unfortunately, definitive answers are not possible at this stage of the calculations and future work is also needed in order to give an appropriate answer, as much experimental work has focussed on CBZ, but very little for any of its derivatives.

4.2 On molecular shape as the most important factor dictating molecular packing

Interestingly, we noticed that not only the hydrogen bond arrangements and the packing motifs but also the observed crystal structures of DHCBZ (the $P2_1/c$ polymorph) and OXCBZ were very similar, if not isostructural (Figure 9). Indeed, if the OXCBZ molecule is replaced by that of DHCBZ in VACTAU01 and lattice energy minimized, the crystal structure of OXCBZ is obtained and vice versa. This is an important observation as, even though the molecular structures of both are different chemically, nearly isomorphic crystals are observed. This highlights the importance of overall molecular shape in determining crystal packing; despite the opportunity for extra hydrogen bonding in OXCBZ (using the carbonyl group), the two geometrically superimposable molecules adopt the same crystal structure. Indeed, the most stable crystal structure in which the carbonyl oxygen does participate in hydrogen bonding is 4.7 kJ/mol less favoured than the experimentally observed crystal. Also, by examining the set of predicted crystal structures of CBZ, we found a crystal structure close to isomorphic with the crystal structure of DHCBZ and OXCBZ (relative energy of about 2 kJ/mol above the monoclinic polymorphs). The growth of this crystal structure was attempted without success by seeding a saturated CBZ solution in ethanol with crystals of DHCBZ.

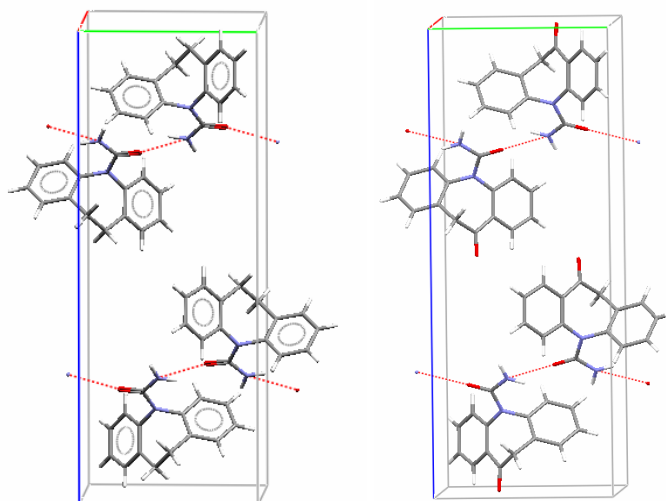


Figure 9. Unit cells of the crystal structures of dihydrocarbamazepine¹⁴ ($P2_1/c$, $a=5.51 \text{ \AA}$, $b=9.16 \text{ \AA}$, $c=24.27 \text{ \AA}$) and oxcarbazepine¹³ ($P2_1/c$, $a=5.28 \text{ \AA}$, $b=9.31 \text{ \AA}$, $c=24.84 \text{ \AA}$).

4.3 On the rationalization of the observed hydrogen bond motifs

As Dunitz and Gavezzotti suggested recently,⁴⁵ a detailed analysis of intermolecular motifs in virtual and experimental crystal structures is a unique way of assessing which motifs are common, which motifs are obligatory and which motifs are unlikely for a certain system. As stated previously, both the CSP and PIXEL calculations indicated that the chain motifs are favoured over anti-dimers in the most stable generated crystal structures of DHCBZ and OXCBCZ (the only molecules where the azepine ring is distorted). This is not the case for CBZ, where chains and anti-dimers are present in the most stable predicted structures, nor for ECBZ where anti-dimers are more popular in the lowest energy region. However, as shown by the PIXEL calculations, the calculated interaction energies of the anti-dimer motifs are very similar in all four cases, i.e. because the structural differences between the molecules are remote from the amide group and they do not affect the dimer interaction. Rather than dimers being energetically

disfavoured for DHCBZ and OXCBZ, it would appear, therefore, that the small changes in molecular shape by the azepine ring distortion favours the chain interaction. But, why do such small changes in molecular shape favour chains over dimers and why has a chain structure not been observed for CBZ, even after a quite extensive experimental screening⁶?

Almost 40 years ago, Kitaigorodskii suggested that the structure of a crystal is mainly dictated by repulsive forces.⁴⁶ If the chain structures of the different crystals are analyzed carefully (Figure 10), important geometric differences can be observed. For similar C_{ar}H--C_{ar} close contacts in all chain structures (Figure 10), the observed OXCBZ and DHCBZ crystals allow the best hydrogen bond contacts, leading to a 5 kJ/mol advantage in Coulombic and polarization energy over chains in CBZ. Furthermore, the predicted N--O distance for the two observed chain structures (OXCBZ and DHCBZ) lie in the highest probability of the N--O distance distribution of amide structures showing hydrogen bonds distinct to dimers in the CSD. In contrast, the N--O distance in the predicted CBZ chain structure lies in the tail of the histogram (Figure 11), suggesting that it is energetically strained.

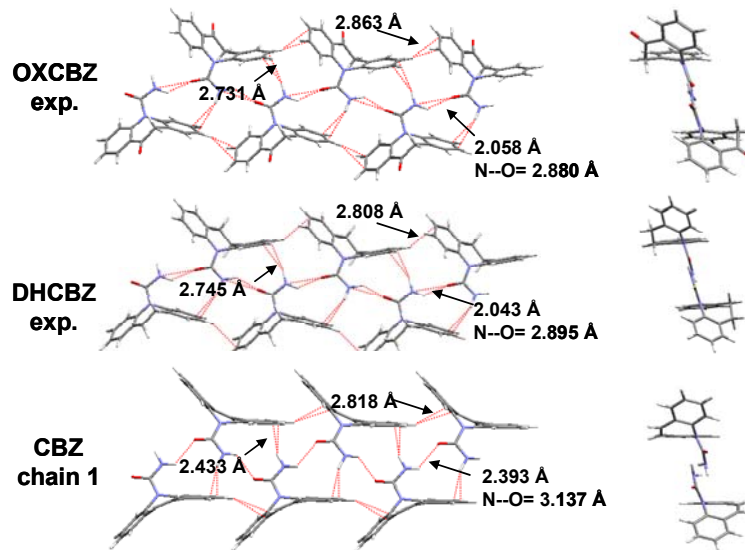


Figure 10. Comparison of the chain structures of the observed OXCBZ and DHCbz crystals and the hypothetical most stable chain structure of CBZ.

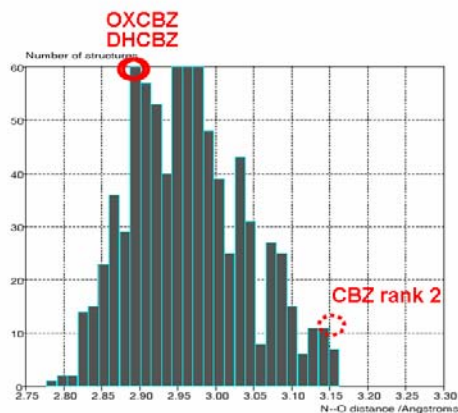


Figure 11. Histograms of N--O distances in the crystal structures of amides (384 entries, excluding dimer motifs) found in the CSD.⁸

As pointed out in Section 3.1, the changes in molecular shape of DHCbz and OXCBZ with respect to CBZ are most important around the azepine ring (Figure 3), since for DHCbz and OXCBZ one of the benzene rings is twisted slightly inwards. This small deformation of the azepine ring allows these two molecules to come closer in the chain structure and thus optimize the hydrogen bonding. Similar optimal hydrogen bonds

cannot be formed in CBZ chains (and neither in ECBZ) without generating very short, repulsive, CH--C close contacts.

This analysis offers an explanation (at least in part) as to why the OXCBZ and DHCBZ chains are more stable than the CBZ chain. Even though the total lattice energy of a chain structure of CBZ is competitive with the observed forms III and IV, the geometrically strained hydrogen bond chains might be at a disadvantage during crystallization. If it was found to be the only stable structure by far, then it would be expected to be found experimentally under certain conditions. However, its accessibility during nucleation is disfavoured, as other isoenergetic crystals showing stronger hydrogen bonding are possible. This may explain why, even after extensive experimental effort,⁶ crystal structures containing chains have not been observed for CBZ.

5. Conclusions

Successful crystal structure prediction (CSP) calculations have been presented for two of the CBZ polymorphs and the crystal structures of OXCBZ and DHCBZ. On the contrary, metastability of the known ECBZ crystal structure is proposed, as both CSP and PIXEL calculations suggest that neither the crystal structure nor the syn-dimer interaction were amongst the most favoured possibilities. Analysis of the low energy calculated crystal structures helps rationalize why the small changes in molecular structure result in completely different hydrogen bonding arrangements in their crystal structures. Complementary, some PIXEL calculations on the different hydrogen bond motifs showed how the small distortion in the azepine rings in DHCBZ and OXCBZ resulted in chain motif preference, as the molecules were able to approach closer and therefore maximize

the hydrogen bond interaction in the hydrogen bonded chains. With a combined CSP and PIXEL calculation study we have shown how, although hydrogen bonds are crucial in the stability of these crystal structures, it is indeed the repulsions and the molecular shape (even if the changes are very small) that dictate the final packing of the structures and, in the end, the hydrogen bonding.

Acknowledgements

We thank Dr Neil Feeder for valuable discussions in this project. We would also thank Dr. James Chisholm for the COMPACK algorithm implemented in COSET and Prof. Angelo Gavezzotti for PIXEL. Finally, we thank the Pfizer Institute for Pharmaceutical Materials Science for funding.

References

- (1) Morselli, P.; Frigerio, A. *Drug Metab. Rev.* **1975**, *4*, 97-113.
- (2) Pellock, J. M. *Epilepsia* **1987**, *28*, S64-S70.
- (3) Schmidt, D.; Elger, C. C. *Epilepsy Behav.* **2004**, *5*, 627-635.
- (4) Shorvon, S. *Seizure* **2000**, *9*, 75-79.
- (5) Grzesiak, A. L.; Lang, M. D.; Kim, K.; Matzger, A. J. *J. Pharm. Sci.* **2003**, *92*, 2260-2271.
- (6) Florence, A. J.; Johnston, A.; Price, S. L.; Nowell, H.; Kennedy, A. R.; Shankland, N. *J. Pharm. Sci.* **2006**.
- (7) Fleischman, S. G.; Kuduva, S. S.; McMahon, J. A.; Moulton, B.; Walsh, R. D. B.; Rodriguez-Hornedo, N.; Zaworotko, M. J. *Cryst. Growth Des.* **2003**, *3*, 909-919.
- (8) Allen, F. H. *Acta Crystallogr. Sect. B: Struct. Sci.* **2002**, *B58*, 380-388.
- (9) Lowes, M. M. J.; Caira, M. R.; Lötter, A. P.; Van Der Watt, J. G. *J. Pharm. Sci.* **1987**, *76*, 744-752.

- (10) Reboul, J. P.; Cristau, B.; Soyfer, J. C.; Astier, J. P. *Acta Crystallogr. Sect. B: Struct. Sci.* **1981**, *37*, 1844-1848.
- (11) Lang, M. D.; Kampf, J. W.; Matzger, A. J. *J. Pharm. Sci.* **2002**, *91*, 1186-1190.
- (12) Cruz Cabeza, A. J.; Day, G. M.; Motherwell, W. D. S.; Jones, W. *Cryst. Growth Des.* **2006**, ASAP article, DOI:101021/cq601756.
- (13) Hempel, A.; Camerman, N.; Camerman, A.; Mastropaolo, D. *Acta Crystallogr. Sect. E: Struct. Rep.* **2005**, *E61*, o1313-o1315.
- (14) Bandoli, G.; Nicolini, M.; Ongaro, A.; Volpe, G.; Rubello, A. *J. Cryst. Spectrosc. Res.* **1992**, 177.
- (15) Bellucci, G.; Chiappe, C.; Marchetti, F. *Gazz. Chim. Ital.* **1995**, *125*, 341-346.
- (16) Lommerse, J. P. M.; Motherwell, W. D. S.; Ammon, H. L.; Dunitz, J. D.; Gavezzotti, A.; Hofmann, D. W. M.; Leusen, F. J. J.; Mooij, W. T. M.; Price, S. L.; Schweizer, B.; Schmidt, M. U.; van Eijck, B. P.; Verwer, P.; Williams, D. E. *Acta Crystallogr. Sect. B: Struct. Sci.* **2000**, *56*, 697-714.
- (17) Motherwell, W. D. S.; Ammon, H. L.; Dunitz, J. D.; Dzyabchenko, A.; Erk, P.; Gavezzotti, A.; Hofmann, D. W. M.; Leusen, F. J. J.; Lommerse, J. P. M.; Mooij, W. T. M.; Price, S. L.; Scheraga, H.; Schweizer, B.; Schmidt, M. U.; van Eijck, B. P.; Verwer, P.; Williams, D. E. *Acta Crystallogr. Sect. B: Struct. Sci.* **2002**, *58*, 647-661.
- (18) Day, G. M.; Motherwell, S.; Ammon, H. L.; Boerrigter, S. X. M.; Della Valle, R. G.; Venuti, E.; Dzyabchenko, A.; Dunitz, J. D.; Schweizer, B.; van Eijck, B. P.; Facelli, J. C.; Bazterra, V. E.; Ferraro, M. B.; Hofmann, D. W. M.; Leusen, F. J. J.; Liang, C.; Pantelides, C. C.; Karamertzanis, P. G.; Price, S. L.; Lewis, T. C.; Nowell, H.; Torrisi, A.; Scheraga, H.; Arnautova, Y. A.; Schmidt, M. U.; Verwer, P. *Acta Crystallogr. Sect. B: Struct. Sci.* **2005**, *61*, 511-527.
- (19) Bernstein, J. *Polymorphism in Molecular Crystals*; Oxford University Press, 2002.
- (20) Bauer, J.; Spanton, S.; Henry, R.; Quick, J.; Dziki, W.; Porter, W.; Morris, J. *J. Pharm. Res.* **2001**, *18*, 859-866.

- (21) Chemburkar, S. R.; Bauer, J.; Deming, K.; Spiwek, H.; Patel, K.; Morris, J.; Henry, R.; Spanton, S.; Dziki, W.; Porter, W.; Quick, J.; Bauer, P.; Donaubauer, J.; Narayanan, B. A.; Soldani, M.; Riley, D.; McFarland, K. *Org. Process Res. Dev.* **2000**, *4*, 413-417.
- (22) Gavezzotti, A. *CrystEngComm* **2003**, *5*, 429-438.
- (23) Gavezzotti, A. *CrystEngComm* **2003**, *5*, 439-446.
- (24) MS Modelling; Release 3.0.1; Accelrys Inc., San Diego, 2004.
- (25) Perdew, J. P.; Wang, Y. *Phys. Rev. B* **1992**, *45*, 13288-13249.
- (26) Delley, B. J. *J. Chem. Phys.* **1990**, *92*, 508-517.
- (27) Williams, D. E. *J. Mol. Struct.* **1999**, *486*, 321-347.
- (28) Williams, D. E. *J. Comput. Chem.* **2001**, *22*, 1154-1166.
- (29) Williams, D. E. *J. Comput. Chem.* **2001**, *22*, 1-20.
- (30) Momany, F. A. *J. Phys. Chem.* **1978**, *82*, 592.
- (31) Cox, S. R.; Williams, D. E. *J. Comput. Chem.* **1981**, *2*, 304.
- (32) Stone, A. J.; Alderton, M. *Mol. Phys.* **1985**, *56*, 1047-1064.
- (33) CADPAC, version 6.0; Amos, R. D.; with contributions from Alberts, I. L.; Andrews, J. S.; Colwell, S. M.; Handy, N. C.; Jayatilaka, D.; Knowles, P. J.; Kobayashi, R.; Koga, N.; Laidig, K. E.; Maslen, P. E.; Murray, C. W.; Rice, J. E.; Sanz, J.; Simandiras, E. D.; Stone, A. J.; Su, M. D.: 1995.
- (34) Karfunkel, H. R.; Gdanitz, R. J. *J. Comput. Chem.* **1992**, *13*, 1171.
- (35) Karfunkel, H. R.; Leusen, F. J. J. *Speedup* **1992**, *6*, 43.
- (36) Verwer, P.; Leusen, F. J. J. *Rev. Comput. Chem.* **1998**, *12*, 327-365.
- (37) Cerius2; version 4.6; Accelrys Inc., A.: San Diego, 1997.
- (38) Day, G. M.; Chisholm, J.; Shan, N.; Motherwell, W. D. S.; Jones, W. *Cryst. Growth Des.* **2004**, *4*, 1327-1340.
- (39) DMAREL; version 3.1; Price, S. L.; Willock, D. J.; Leslie, M.; Day, G. M.: 2001.
- (40) Chisholm, J. A.; Motherwell, S. *J. Appl. Crystallogr.* **2005**, *38*, 228-231.
- (41) Gavezzotti, A. *Z. Kristall.* **2005**, *220*, 499-510.
- (42) Harrison, W. T. A.; Yathirajan, H. S.; Anilkumar, H. G. *Acta Crystallogr. Sect. C: Cryst. Struct. Commun.* **2006**, *C62*, o240-o242.

- (43) Gelbrich, T.; Hursthouse, M. B. *CrystEngComm* **2006**, *8*, 448-460.
- (44) Oswald, I. D. H.; Allan, D. R.; Day, G. M.; Motherwell, W. D. S.; Parsons, S. *Cryst. Growth Des.* **2005**, *5*, 1055-1071.
- (45) Dunitz, J. D.; Gavezzotti, A. *Cryst. Growth Des.* **2005**, *5*, 2180-2189.
- (46) Kitaigorodskii, A. I. *Molecular Crystals and Molecules*; Academic Press: New York and London, 1973.